Neuron, Vol. 41, 389–404, February 5, 2004, Copyright ©2004 by Cell Press

Kv1.3 Channel Gene-Targeted Deletion Produces "Super-Smeller Mice" with Altered Glomeruli, Interacting Scaffolding Proteins, and Biophysics

D.A. Fadool,[1,*] K. Tucker,[1] R. Perkins,[2] G. Fasciani,[1] R.N. Thompson,[1] A.D. Parsons,[3] J.M. Overton,[3] P.A. Koni,[4,7] R.A. Flavell,[4,5] and L.K. Kaczmarek[6]

[1]Department of Biological Science
Programs in Neuroscience and Molecular Biophysics
[2]Department of Biological Science
Biomedical Research Facility
[3]Department of Nutrition, Food, and Exercise Science
Program in Neuroscience
The Florida State University
Tallahassee, Florida 32306
[4]Section of Immunobiology and
[5]Howard Hughes Medical Institute
Yale University School of Medicine
New Haven, Connecticut 06520
[6]Departments of Pharmacology and Cellular and Molecular Physiology
Yale University School of Medicine
New Haven, Connecticut 06520

Summary

Mice with gene-targeted deletion of the Kv1.3 channel were generated to study its role in olfactory function. Potassium currents in olfactory bulb mitral cells from Kv1.3 null mice have slow inactivation kinetics, a modified voltage dependence, and a dampened C-type inactivation and fail to be modulated by activators of receptor tyrosine signaling cascades. Kv1.3 deletion increases expression of scaffolding proteins that normally regulate the channel through protein-protein interactions. *Kv1.3*$^{-/-}$ mice have a 1,000- to 10,000-fold lower threshold for detection of odors and an increased ability to discriminate between odorants. In accordance with this heightened sense of smell, *Kv1.3*$^{-/-}$ mice have glomeruli or olfactory coding units that are smaller and more numerous than those of wild-type mice. These data suggest that Kv1.3 plays a far more reaching role in signal transduction, development, and olfactory coding than that of the classically defined role of a potassium channel—to shape excitability by influencing membrane potential.

Introduction

Modulation of voltage-dependent potassium ion channels (Kv channels) via tyrosine phosphorylation can dramatically alter neuronal excitability by modifying the biophysical properties of the channel, its trafficking to subcellular locations, and its level of expression, as well as its ability to participate with scaffolding proteins in multicomplex associations (Huang et al., 1993; Kim et al., 1995; Jonas and Kaczmarek, 1996; Scannevin and Trimmer, 1997; Fadool and Levitan, 1998; Cayabyab et al., 2000; Jugloff et al., 2000; Rogalski et al., 2000; Tiffany et al., 2000; Wong et al., 2002; Rivera et al., 2003). Kv1.3, a member of the *Shaker* family of Kv channels (Yellen, 2002), carries a large proportion of the outward current in mitral and granule cells of the olfactory bulb (OB) (Fadool and Levitan, 1998). In general, Kv channels in the OB are thought to contribute to the resting membrane potential, determine the frequency of repetitive firing, and influence the interspike interval. Multiple tyrosine kinase signaling cascades converge at the level of the Kv1.3 channel, altering its biophysical properties by phosphorylation of multiple but distinct combinations of tyrosine residues (Bowlby et al., 1997; Fadool et al., 1997, 2000; Fadool and Levitan, 1998). Interestingly, at a higher level of complexity, their effects on channel modulation can be altered by sensory deprivation induced by unilateral naris-occlusion, by food restriction, by the duration of kinase activation, and by the repetoire of adaptor proteins expressed in a given olfactory bulb neuron (OBN) cell type (Fadool et al., 2000; Tucker and Fadool, 2002; Cook and Fadool, 2002).

Because of this complex convergence of modulation at a single channel protein and the marked state dependency of its modulation, we have examined mice with gene-targeted deletion of the Kv1.3 channel (*Kv1.3*$^{-/-}$) to understand its contribution to olfactory function. Olfactory neurons from Kv1.3 null mice have modified action potentials and altered potassium currents that fail to be modulated by activators of receptor tyrosine kinases, insulin and brain-derived neurotrophic factor (BDNF). Deletion of the Kv1.3 channel also increases the expression of its modulatory and interacting proteins of tyrosine kinase signaling cascades. Moreover, the mice have a heightened sense of smell. Image analysis of the OB indicates that the glomeruli, the olfactory coding units of the bulb, are smaller and more numerous in *Kv1.3*$^{-/-}$ mice than in wild-type animals (+/+). Thus the Kv1.3 ion channel may regulate the kinetics and timing of neuronal responses to repetitive stimulation, and its absence changes the structure of OB glomeruli and modifies the capacity to detect odorant molecules.

Results

Electrophysiological Analysis of OBN Current in Kv1.3 Null Mice

Kv1.3 null (−/−) mice were generated previously by deleting a large promoter region and the N-terminal third of the Kv1.3 coding sequence (Xu et al., 2003; Koni et al., 2003). To characterize the effect of Kv1.3 deletion on the electrical properties of olfactory neurons, cultured OB mitral cells were first voltage clamped in the whole-cell configuration at −90 mV and stepped in 5 mV depolarizing increments to +40 mV. With our defined patch-recording solutions, Kv1.3 carries 60%–80% of

*Correspondence: dfadool@bio.fsu.edu
[7]Present address: Institute of Molecular Medicine and Genetics, Department of Medicine, Medical College of Georgia, Augusta, Georgia 30912.

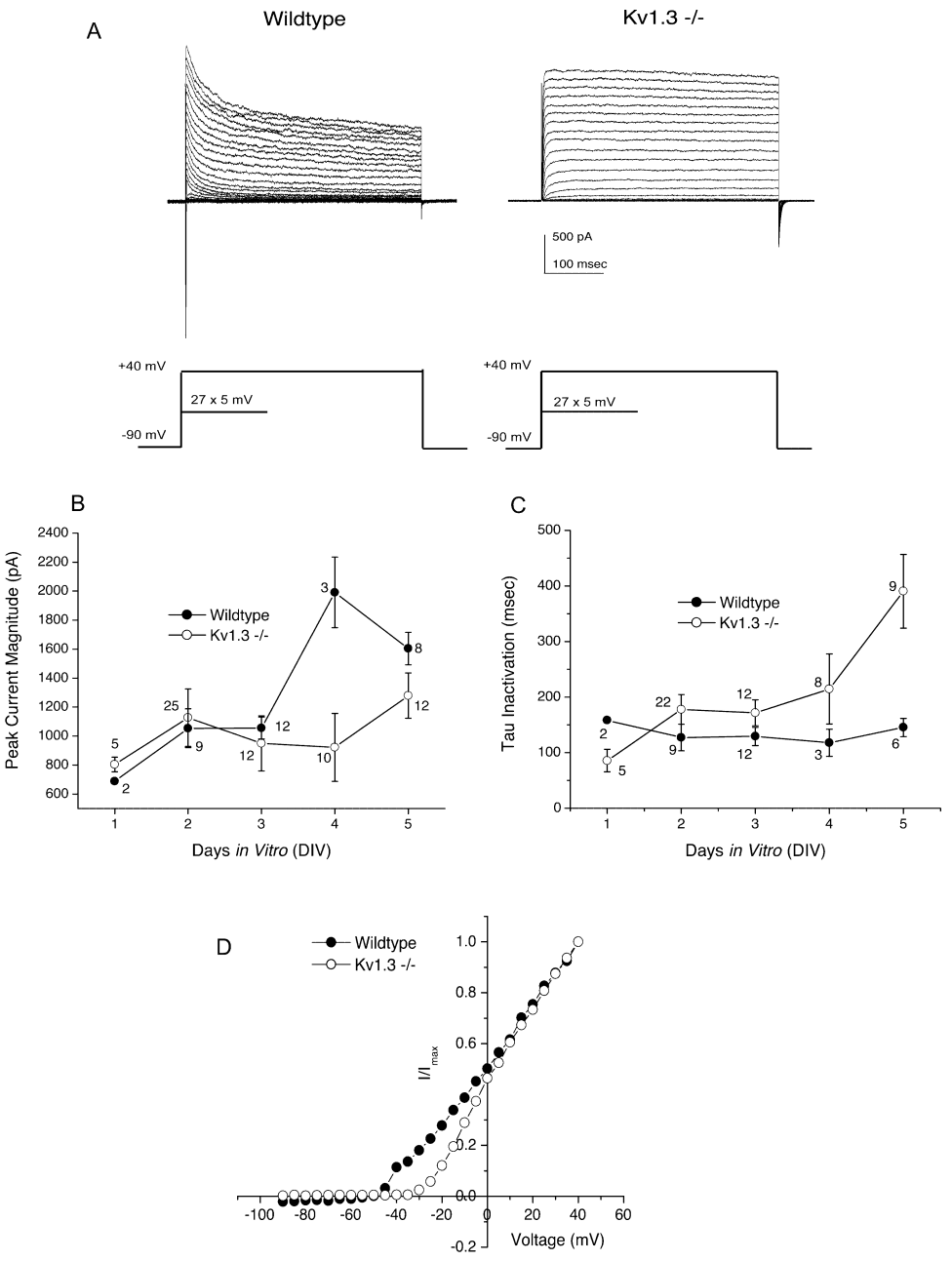

Figure 1. Whole-Cell Voltage-Clamp Currents in Mitral Cells of the Olfactory Bulb from Wild-Type and Kv1.3 Null Mice

(A) Representative records from a mitral cell voltage clamped in the whole-cell configuration taken from olfactory bulb neurons (OBNs) cultured from wild-type or Kv1.3 null mice (*Kv1.3*$^{-/-}$). Neurons were held at −90 mV (V_h) and stepped in 5 mV increments (V_c) to a final potential of +40 mV. The duration of pulses was 1000 ms with a 45 s interpulse interval to prevent cumulative inactivation of the Kv1.3 channel. Both recordings are from mitral cells that were 5 days in vitro (DIV5).

(B) Peak current magnitude from neurons that were held at −90 mV (V_h) and stepped to a single depolarizing potential of +40 mV (V_c) is plotted against days in vitro (DIV). Duration and interpulse interval of the voltage paradigm was the same as in (A). ●, wild-type; ○, Kv1.3 null mice. Mean ± SEM with sample size (n) as noted.

(C) Same as in (B) but for the kinetics of inactivation (τ) plotted against DIV.

(D) Normalized current-voltage relation for a representative family of currents evoked by stimulating a wild-type and Kv1.3 null neuron with the paradigm in (A). I, current in pA; I_{max}, maximal current at +40 mV. Both recordings are from mitral cells that were DIV 5 and are representative of twelve such plots of each genotype.

the outward current as determined pharmacologically by margatoxin sensitivity in rat or mouse OBNs (Fadool and Levitan, 1998; Colley et al., 2004). Pharmacological elimination of this component of outward current would be expected to leave a more rapidly inactivating component of A-type current that has been attributed to the Kv1.4 subunit (Fadool and Levitan, 1998). In contrast, however, we found that the mitral cell inactivation time

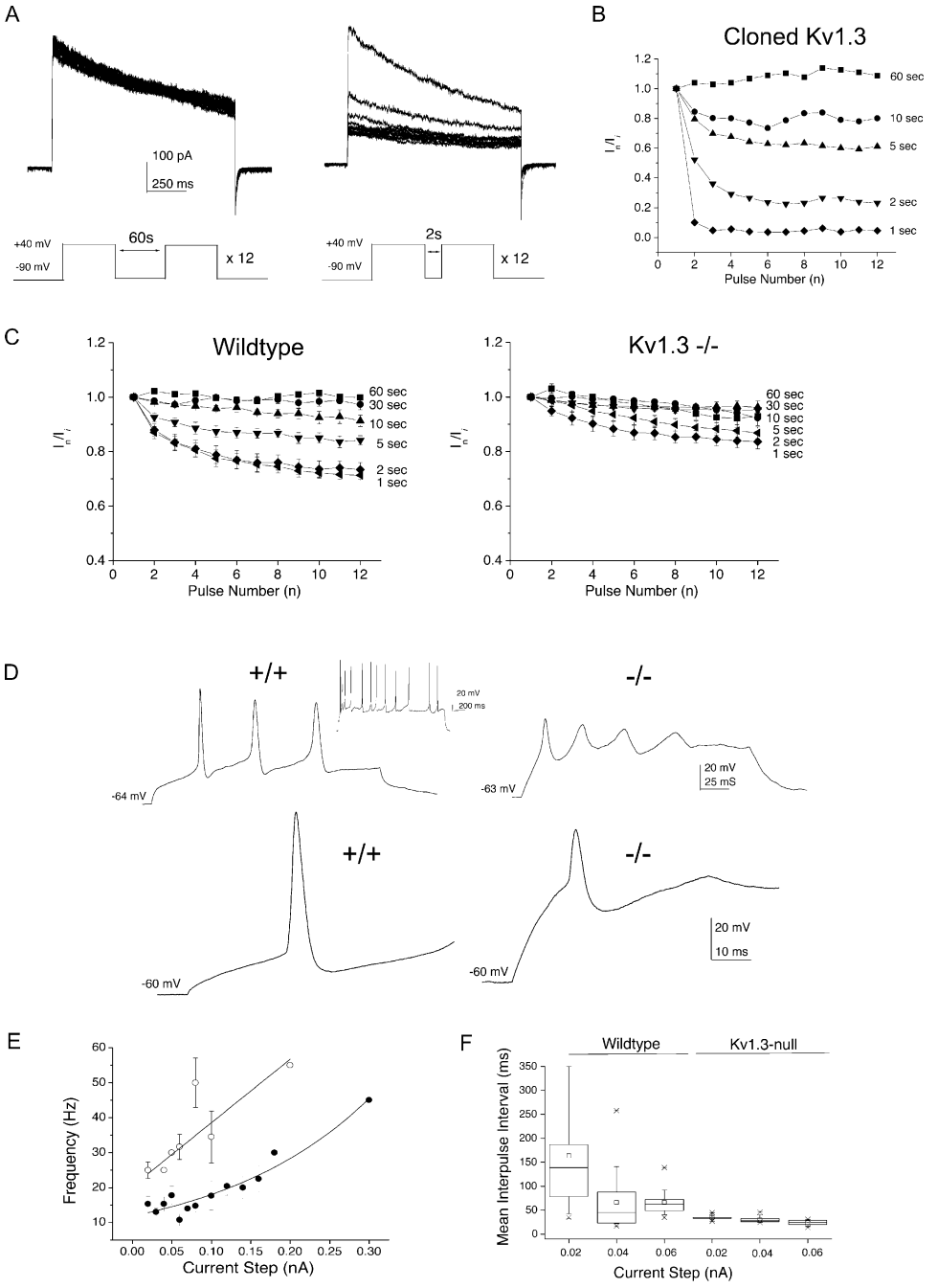

Figure 2. Cumulative Inactivation Kinetics, Evoked Activity, and Action Potential Shape Are Altered in Olfactory Bulb Neurons of Kv1.3 Null Mice

(A) Human embryonic kidney (HEK293) cells were transiently transfected with Kv1.3 cDNA and recorded in the cell-attached configuration after 48 hr. Representative macroscopic currents for a patch held (V_h) at −90 mV and stepped twelve times to a single depolarizing step (V_c) of +40 mV with an interpulse interval of 60 s (left) or 2 s (right).

(B) Plot of the normalized current magnitude measured at the Nth pulse number over that of the initial pulse (I_n/I_i) for the protocol described above. Interpulse intervals noted at the right of each plot.

(C) Same as (A) and (B) but for normalized whole-cell currents recorded from native mitral cells cultured from wild-type (Wild-type; left) or Kv1.3 null mice (*Kv1.3*$^{-/-}$; right). DIV 5. Sample size = 6–8; mean ± SEM.

(D) (Top) Representative current-clamp recordings from mitral cells cultured from wild-type (+/+; left) or Kv1.3 null mice (−/−; right). Neurons were injected with a depolarizing current step (0.02 nA, 200 ms) to evoke a train of action potentials in these cells. Membrane potential was held at the voltage indicated above each trace. (Inset) Same neuron injected with a current step of 1000 ms duration. (Bottom) Enlarged scale for the first action potential evoked in the trains above. Same notation as in top portion (D). DIV 9.

(E and F) Action potential firing frequency (E) and interpulse interval (F) were compared between neurons from wild-type (●) and Kv1.3 null mice (○) using the first overshooting action potential of a train of action potentials as recorded in (D). DIV 9–10. Sample size = 28–30 neurons per genotype; mean ± SEM.

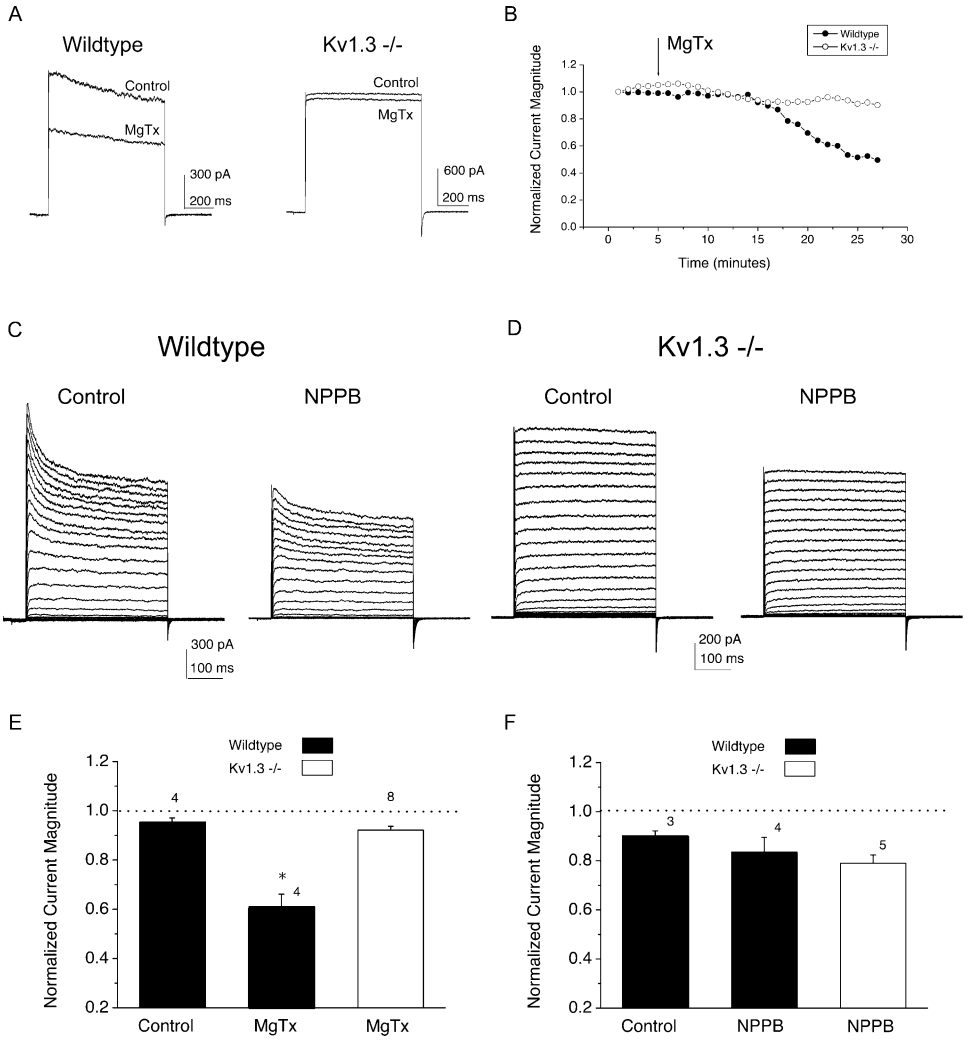

Figure 3. Kv1.3 Sensitivity to the Scorpion Toxin, Margatoxin, and a Nonselective Chloride Channel, NPPB

(A) Representative whole-cell currents from mitral cells of wild-type and Kv1.3 null mice that were stepped to a single depolarizing voltage of +40 (V_c) mV from a holding potential (V_h) −90 mV in 1 min interpulse intervals. Control, time 0; MgTx, 20 min post bath application of 50 pM MgTx.

(B) Normalized current magnitude plotted against time, demonstrating the expected slow on-rate of channel block. MgTx was applied at the arrow. DIV 4.

(C) Same voltage protocol as in Figure 1. Control, time 0; NPPB, 20 min post bath application of 100 μM NPPB. DIV 6.

(D) Same as in (C) but for Kv1.3 null mice.

(E) Summary histograms of the normalized current magnitude for vehicle treated (bath saline or 0.1% EtOH in bath saline) versus toxin treated cells for MgTx (left) and NPPB (right). Mitral cells from wild-type (■) or Kv1.3 null (□) mice were held (V_h) at −90 mV and stepped to a single depolarizing voltage of +40 mV (V_c) with 1 min interpulse intervals. DIV 4–6. Mean ± SEM; sample sizes as indicated; *, significantly different, $\alpha \leq 0.05$, paired t test. Dashed line, no change in current magnitude upon application of either vehicle (Control) or toxin (MgTx, NPPB) for 20 min.

constant (τ_{Inact}) was greatly slowed in Kv1.3 null mice relative to that in wild-type animals (Figure 1A). Mitral cells from Kv1.3 wild-type mice had a steady τ_{Inact} of 100–150 ms independent of days in vitro (DIV), in contrast to those from Kv1.3 null mice, in which τ_{Inact} increased progressively over DIV to reach over 400 ms by DIV 5 (Figure 1C). Although both genotypes expressed the same outward current magnitude when initially placed into primary cell culture, by DIV 4–5 the null mice failed to express currents greater than about 1200 pA, whereas their time-matched wild-type controls reached between 1600 and 2200 pA (Figure 1B). Independent of DIV, Kv1.3 null mice also have an altered voltage dependence of activation. The threshold for activation of the outward, whole-cell current in mitral cells from Kv1.3 null mice is shifted by approximately +20 mV in the positive direction (Figure 1D).

Cumulative Inactivation Is Altered in the OBNs of Kv1.3 Null Mice

One of the characteristics of Kv1.3 channels is that their rate of exit from the inactivated state is extremely slow, a property that contributes to cumulative inactivation when the channel is depolarized repetitively (Marom and Levitan, 1994). Thus, a repeated interpulse interval shorter than 30 s causes a build-up of channels in the

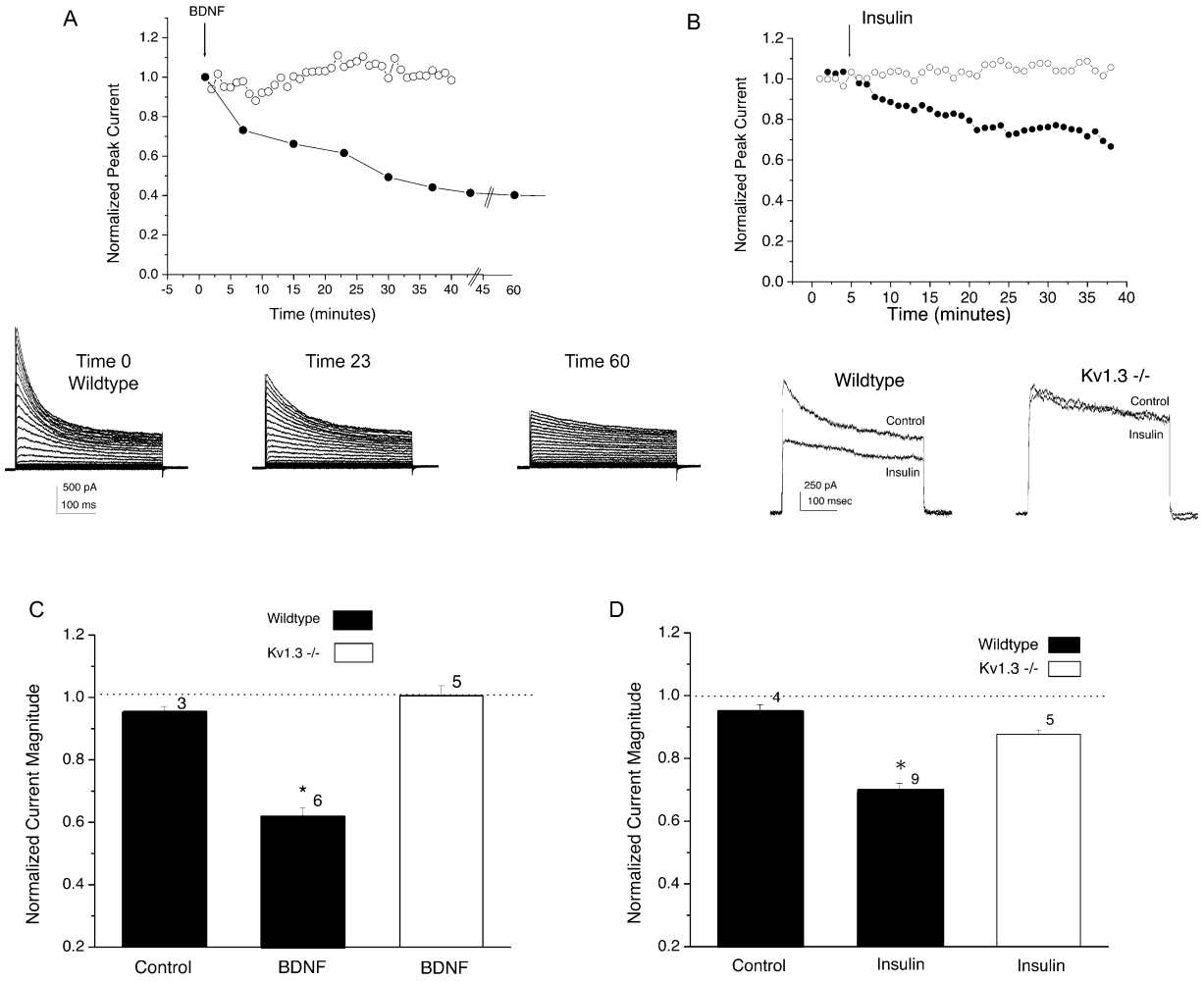

Figure 4. Kv1.3 Null Mice Are Insensitive to Known Receptor Tyrosine Kinase Modulators of the Channel

(A) Normalized whole-cell current magnitude is plotted against time for a representative mitral cell held at −90 mV (V_h) and stepped either to a single depolarizing potential of +40 mV (V_c) or stimulated with the voltage protocol in Figure 1. Fifty nanogram of BDNF was bath applied at time 3 min (arrow). ○, wild-type; ●, Kv1.3 null mice. Representative recordings demonstrating the time course of current suppression in wild-type neurons by BDNF is shown below. Voltage protocol as in Figure 1; BDNF application at time 3 min. DIV 5.

(B) Same as in (A) but for bath application of 1 μg/ml insulin at time 5 min. Representative recordings demonstrating two time points, before and after current suppression, in wild-type and Kv1.3 null neurons, are shown below. Control, time 0; Insulin, 20 min after bath application. DIV 4.

(C) Summary histogram for BDNF-treated neurons as described in (A). Mitral cells from wild-type (■) or Kv1.3 null (□) mice were held (V_h) at −90 mV and stepped to a single depolarizing voltage of +40 mV (V_c) in 1 min interpulse intervals. Mean ± SEM; sample sizes as indicated; *, significantly different, $\alpha \leq 0.05$, paired t test. Dashed line, no change in current magnitude upon application of either vehicle (Control) or tyrosine kinase (BDNF) for 20 min. DIV 4–5.

(D) Same as in (C) but for insulin.

inactivated state and results in progressive reduction of the macroscopic outward current. Figures 2A and 2B demonstrate this property for human embryonic kidney cells (HEK293 cells) transiently transfected with Kv1.3 cDNA. The patch was held at −90 mV and stepped 12 times to +40 mV for 1 s with interpulse intervals from 60 to 1 s. Figure 2A is a representative recording with a 60 s interpulse interval (left) or a 2 s interpulse interval (right), and Figure 2B is a plot of the degree of inactivation at different intervals for this cell. We have previously demonstrated that Src kinase disrupts this cumulative inactivation, which can be partially restored by the Grb but not the Shc adaptor molecule (Cook and Fadool, 2002). Because both Src and the adaptor protein Grb are expressed in the wild-type OB (see Figure 7B), we may expect that wild-type mitral cells would demonstrate an intermediate perturbation in the degree of cumulative inactivation of Kv1.3 current. Using the same voltage protocol and analysis described above, this is indeed what was observed for the wild-type neurons (Figure 2C). In mitral cells from the Kv1.3 null animals, however, no cumulative inactivation was observed until the interpulse interval was shortened to as little as 1–2 s, and even then, 90% of the channels were available for restimulation to the open state.

Action Potentials Are Altered in the OBNs of Kv1.3 Null Mice

The membrane excitability of 58 mitral cells (30 wild-type, 28 Kv1.3 null) was investigated by injecting super-

Table 1. Comparison of Whole-Animal Physiological Properties in Wild-Type and Kv1.3 Null Mice as Monitored in Metabolic Chambers for 8 Days

Property	Wild-Type Mice (n = 10)	Kv1.3 Null Mice (n = 10)
Body weight (g)	27.3 ± 0.7	*24.4 ± 0.6
Caloric intake (kcal)	17.2 ± 1.8	15.9 ± 2.0
Number of food events		
12 hr dark	168 ± 32	*293 ± 47
10 hr light	63 ± 14	118 ± 30
Water intake (g)	6.5 ± 0.4	5.6 ± 0.3
Number of licks		
12 hr dark	3597 ± 246	*2123 ± 176
10 hr light	938 ± 144	*505 ± 92
Normalized VO_2 (ml/min/kg$^{0.75}$)		
12 hr dark	31.5 ± 1.0	33.5 ± 0.8 (37.1; first 12 hr)
10 hr light	25.3 ± 0.8	26.5 ± 0.7
Locomotor activity (m)		
12 hr dark	285 ± 47	*468 ± 98
10 hr light	81 ± 11	134 ± 24

Values are means ± SEM. Body weight and caloric and water intakes were measured daily during a 2 hr maintenance period just before lights off. All other measures were derived from continuous data collection over 8 days accumulated in 30 s intervals and separated into 12 hr dark and 10 hr light period means. *, Significantly different by Student's t test, $\alpha \leq 0.05$.

threshold current pulses while holding the neurons near or below the resting potential. Only neurons with resting potentials of at least −50 mV were considered in the analysis. The resting potential of the mitral cells from Kv1.3 null mice (−55.5 ± 1.0 mv) was slightly more depolarized than that from wild-type mice (−57.9 ± 1.3 mv; $\alpha \leq 0.05$, Student's t test). Wild-type neurons typically responded to intracellular current injection by repetitive firing of action potentials (Figure 2D) that was variable in interspike interval (Figure 2D, inset; Figure 2F). Neurons from Kv1.3 null mice fired a leading action potential of lower amplitude than that of wild-type mice, followed by action potentials of decreasing amplitude at a regular and higher frequency than wild-type (Figures 2E and 2F). A comparison of action potentials across the two genotypes demonstrates that those in Kv1.3 null neurons have a lower height (97.6 ± 1.9 mV +/+ versus 63.8 ± 5.2 mV −/−), faster 10%–90% rise time (21.6 ± 0.8 ms +/+ versus 11.5 ± 1.5 ms −/−), greater width at 50% amplitude (3.4 ± 0.1 ms +/+ versus 9 ± 1.4 ms −/−), longer duration (5.8 ± 0.2 ms +/+ versus 7.0 ± 0.6 ms −/−), and lower peak amplitude (31.0 ± 1.3 mV +/+ versus 2.8 ± 4 mV −/−).

Margatoxin-Sensitive Current Is Eliminated in the OBNs of Kv1.3 Null Mice

Margatoxin (MgTx) is believed to be a specific blocker of the Kv1.3 channel. To test for sensitivity to this agent, mitral cells from wild-type and Kv1.3 null mice were stepped to +40 (V_c) from a holding potential (V_h) of −90 mV at 1 min interpulse intervals (Figure 3). At the fifth voltage step, MgTx was applied to the bath (Figure 3B). Peak current magnitude prior to toxin application (time 5) was compared with that 20 min post toxin treatment (time 25) using a within-cell comparison (Figure 3A). MgTx significantly suppressed mitral cell current in wild-type animals but did not affect that from Kv1.3 null mice (paired t test, $\alpha \leq 0.05$, n = 4–8). As a control for patch stability over time, cells were also treated with vehicle control (bath saline in the case of MgTx) to ascertain that there was no significant decay in peak current magnitude over the course of the testing period (Figure 3E). These data indicate that, as expected, loss of the Kv1.3 channel renders neurons insensitive to a specific Kv1.3 channel blocker.

In a recent study of T lymphocytes derived from Kv1.3-deficient mice, an upregulation of a Cl^- conductance was found to compensate for the lack of Kv1.3 current, potentially underlying a stabilization of the resting potential (Koni et al., 2003). Although we did not observe an increase in protein expression for either the ClC_2 or ClC_3 chloride channels in the OB (see below), we also tested this possibility for mitral cells using the non selective Cl channel blocker NPPB. A 20 min application of NPPB produced a small suppression of mitral cell peak current in both wild-type and Kv1.3 null mice, potentially demonstrating an equal contribution of Cl conductance in both genotypes (Figures 3C and 3D). However, the vehicle alone (EtOH) also produced a small suppression of current. Thus, although the response to NPPB was similar for both genotypes, it was not robust or statistically significant (Figure 3F).

Responses to Insulin and BDNF Are Eliminated in the OBNs of Kv1.3 Null Mice

The Kv1.3 null mice additionally provided an opportunity to test the selectivity of receptor tyrosine kinase modulation of Kv current in native neurons for the Kv1.3 *Shaker* channel over other family members also expressed in the same neurons. We hypothesized that if previously reported current suppression of mitral cells by activation of insulin and TrkB tyrosine kinases (Fadool et al., 2000; Tucker and Fadool, 2002) is selective for only Kv1.3 (and not Kv1.4, Kv1.5), then application of the hormones insulin or BDNF would not affect current magnitude in Kv1.3 null mice. Twenty minutes of bath application of either insulin or BDNF significantly suppressed about 30%–40% of the outward current in wild-type animals and had no effect on peak current magnitude of mitral cells from Kv1.3 null mice (Figures 4A–4D; paired t test, $\alpha \leq 0.05$, n = 5–9).

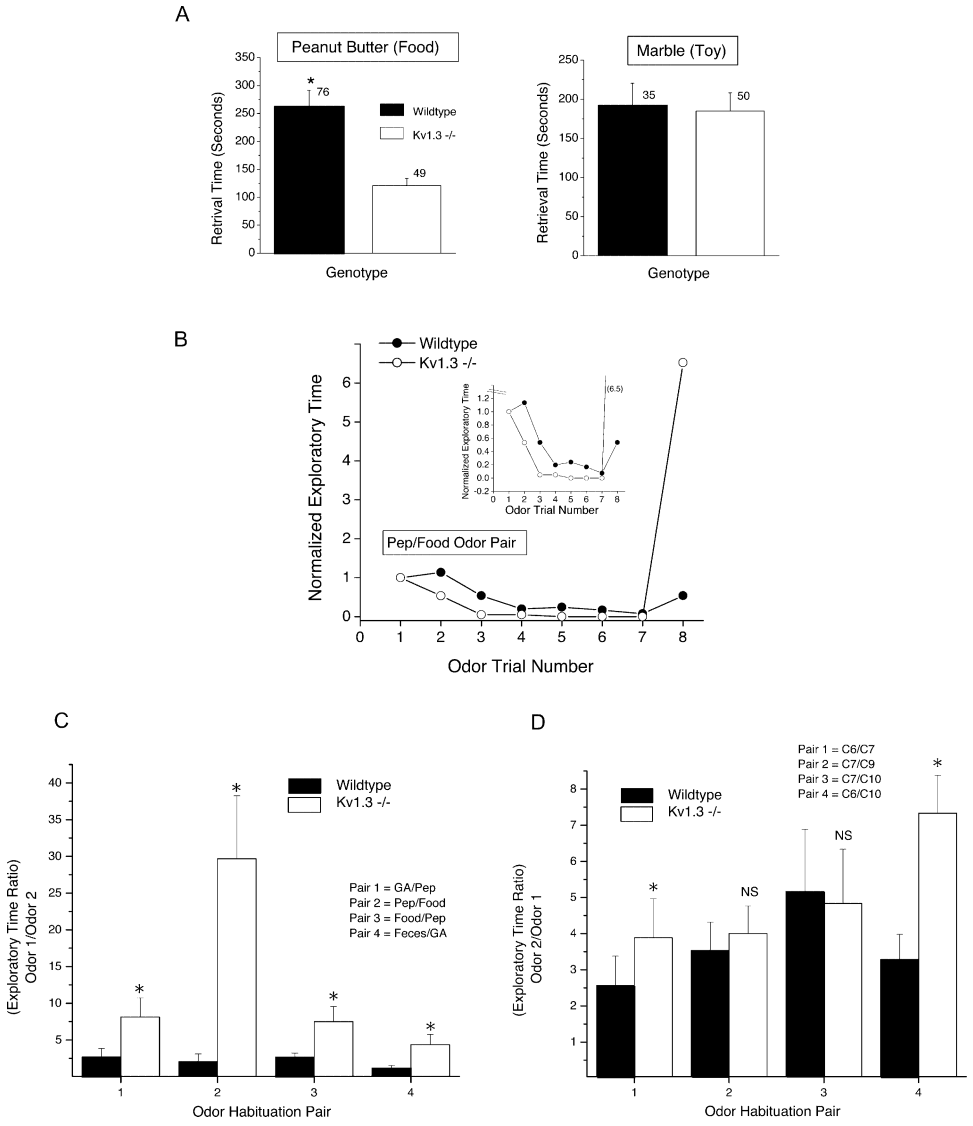

Figure 5. Olfactory Discrimination Is Accessed in Behavioral Tests for Retrieval and Habituation

(A) Histogram plot of the retrieval time in seconds for naive wild-type and Kv1.3 null mice to uncover a hidden food item (peanut butter cracker) or similarly sized item without associated odor (marble). ■, wild-type mice; □, *Kv1.3*$^{-/-}$. Plotted are mean ± SEM, sample sizes (n) as indicated, with statistical significance defined at the 95% confidence level (*), Student's t test.

(B) Plot of the normalized exploratory time versus odor trial number for animals habituated to the first odorant in an odor pair by repeated presentation of the odor at 1 min intervals (see Experimental Procedures). On the eighth trial, the novel, second odorant of the pair is presented to test for discrimination following habituation to the first odorant of the pair. Plotted is a representative trial between a wild-type (●) and *Kv1.3*$^{-/-}$ (○) mouse. Inset shows an expanded lower time scale to provide better resolution of the onset rate of odor habituation. *Kv1.3*$^{-/-}$ mice habituated slightly more rapidly than that of wild-type mice; however, the magnitude of habituation was not different. Pep, peppermint extract (1:100); Food, ground rodent chow extract (see Experimental Procedures).

(C) Histogram plot of the exploratory time following odor habituation (Odor 1) over time spent upon presentation to the novel odor (Odor 2). A ratio value of 1.0 indicates failure to detect the novel odor as different than the habituated odor (zero discrimination). Plotted are mean ± SEM, sample sizes (n) as indicated, with statistical significance defined at the 95% confidence level (*), Student's t test with arc-sin transformation for percentile data. Pep, peppermint extract; Food, ground rodent chow extract; Feces, ground feces extract from caecotroph matter; GA, geranyl acetate. All odorants are 1:100.

(D) Same as in (C) but testing odorant discrimination between alcohol odorant molecules having single C chain differences in length. C6, ethyl butyrate; C7, ethyl valerate; C9, ethyl heptanoate; C10, ethyl caprylate. All odorants are 1:100.

Behavioral and Metabolic Phenotype of Kv1.3 Null Mice

Mice were housed in metabolic chambers for continuous monitoring of O_2 consumption and general activity including locomotor, eating, and drinking behaviors (see Table 1 and Supplemental Figures S1 and S2 at http://www.neuron.org/cgi/content/full/41/3/389/DC1). As previously reported by Xu et al. (2003), the body weight of the Kv1.3 null mice was less than that of the wild-type mice even though total caloric and water intake were not different. Unlike Xu et al. (2003), the level of oxygen consumption normalized to body weight (metabolism)

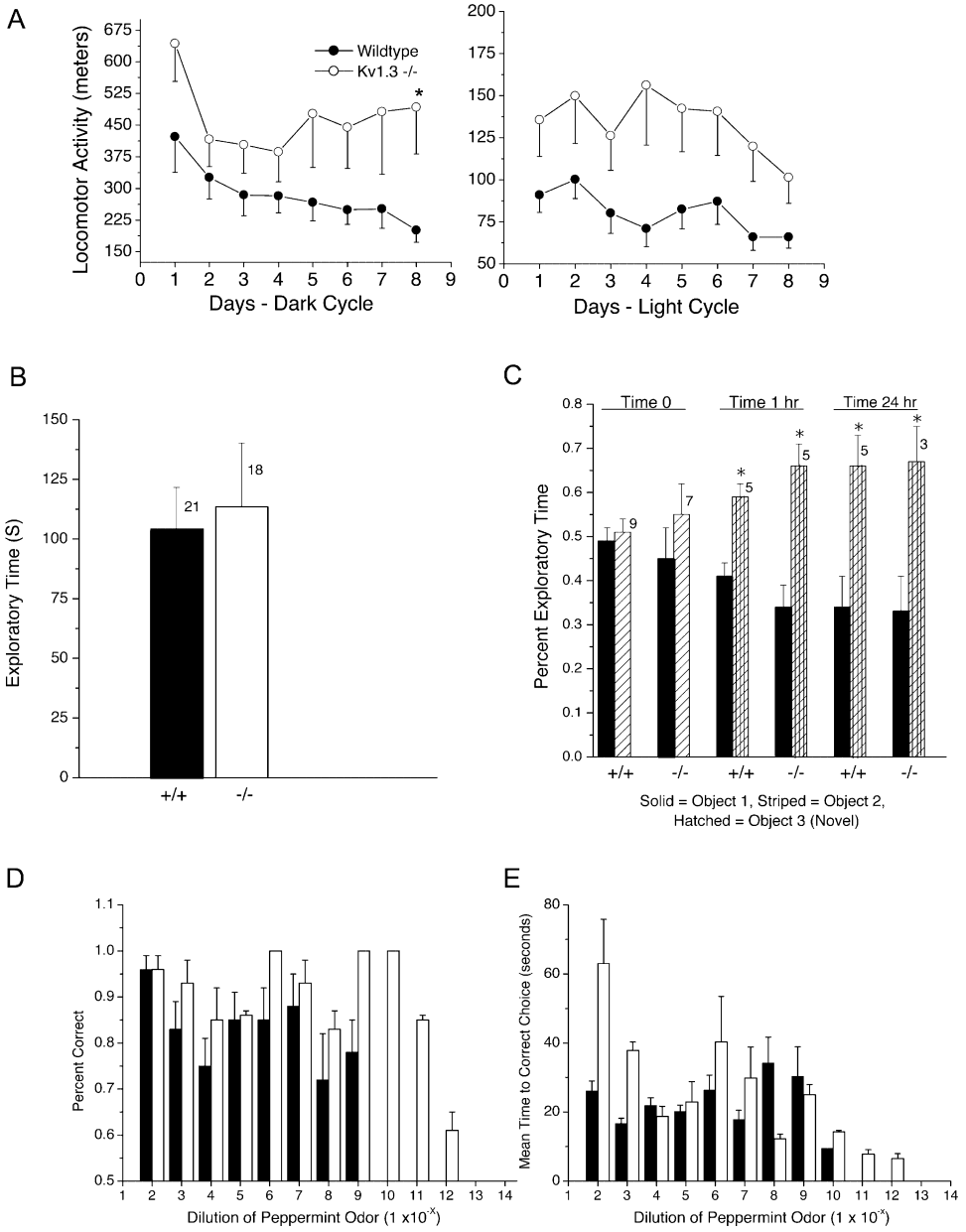

Figure 6. Locomotor Activity, Memory, Exploratory Motivation, and Odorant Threshold Are Accessed in Behavioral Tests Using a Force Platform, Novel Object Recognition, Object Exploration, and a Two-Choice Discrimination Apparatus

(A) Total locomotor activity for wild-type (wild-type, ●) and Kv1.3 null mice (*Kv1.3*$^{-/-}$, ○) is plotted against days and separated into 12 hr dark (right) and 10 hr light (left) periods. Activity was measured using a custom-designed force platform that accumulated activity in 30 s periods and stored distance within a 1 mm resolution. Plotted is the mean of ten animals ± SEM; *, statistical difference in locomotor activity between genotypes using a two-way randomized design ANOVA with *snk* post hoc test; defined at the 95% confidence level.

(B) Basal motivation for exploration is shown by plotting mean exploratory time for a novel object for wild-type (+/+) and Kv1.3 null (−/−) mice. Plotted are mean ± SEM for exploratory times scored during a 5 min interval. Sample sizes (n) of naive mice as indicated; no significant difference by Student's t test at the 95% confidence level.

(C) Novel object recognition test results are plotted for wild-type (+/+) and Kv1.3 null (−/−) mice to determine short- and longer-term memory. Percent exploratory time of object 1 (solid bar) versus object 2 (striped bar) is equivalent (0.5%) for each genotype upon initial presentation of the objects (Time 0). Percent exploratory time of two objects following introduction of novel object 3 (hatched bar) to replace object 2 is plotted for a test group of mice tested 1 hr (time 1 hr) or 24 hr (time 24 hr) after initial object presentation. Plotted are mean ± SEM, sample sizes (n) as indicated, with statistical significance defined at the 95% confidence level (*), Student's t test with arc-sin transformation for percentile data.

(D) The retrieval of a hidden food reward buried under peppermint-scented litter in a two-choice paradigm was used to access odor threshold in wild-type (solid bars) and Kv1.3 null mice (open bars). Percent correct decision was plotted against relative odorant concentration, where odorant was sequentially diluted by 10-fold as indicated on the ordinate. Fifty percent correct (0.5) was defined as the threshold for odorant detection, whereby the animal's decision to dig (indication of choice) was equivalent to chance alone. Data represent the percent mean correct decision ± SEM for ten animals that were trained for each genotype. See text for experimental details.

(E) Same experimental paradigm and notation as (D) but plotting time to correct choice.

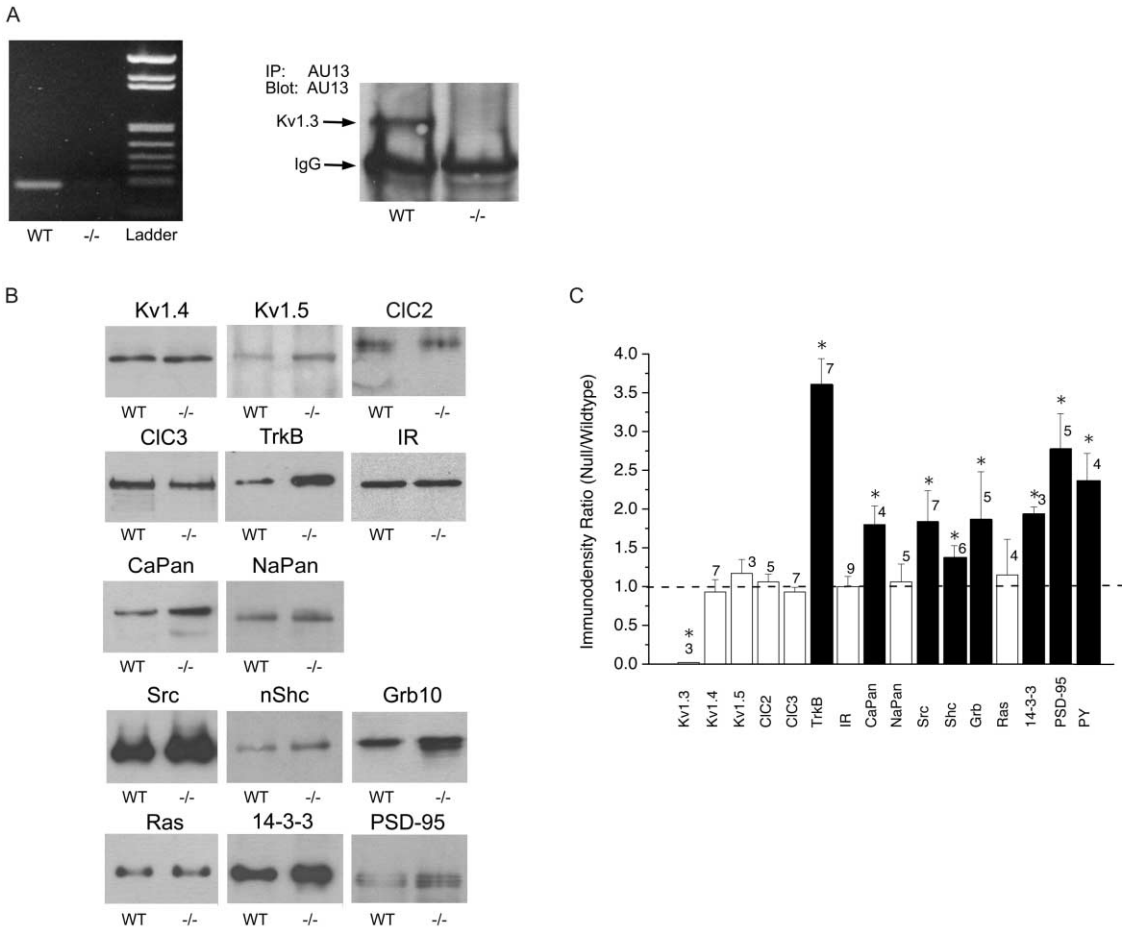

Figure 7. OB Expression Levels of Adaptor, Scaffolding, and K Channel Interacting Proteins in Wild-Type versus Kv1.3 Null Mice

(A) (Left) RT-PCR determination of an expected 184 bp product (see Experimental Procedures) is present in the OB of wild-type mice (WT) but fails to be detected in that of Kv1.3 null mice (−/−) by 1% agarose gel electrophoresis. (Right) P20 OB lysates were used to immunoprecipitate Kv1.3 channel protein using a polyclonal antisera (IP: AU13) against the amino terminus of the channel. Immunoprecipitates were separated by 10% SDS PAGE, electrotransferred to nitrocellulose, and blotted with αAU13 (Blot: AU13). Epichemiluminesense (ECL) was used to visualize the expected Kv1.3 protein between 55 and 72 kDa (arrow). IgG arrow, heavy chain of the immunoglobulin. WT, wild-type; −/−, Kv1.3 null mice.

(B) OB membrane proteins (to probe for Kv1.3, Kv1.4, Kv1.5, ClC_2, ClC_3, CaPan, NaPan, TrkB, IR) and NP40 solubilized proteins (to probe for Shc, Src, Grb10, Ras, 14-3-3, PSD95) were separated by 8%–10% SDS PAGE, electrotransferred to nitrocellulose, and blotted with various antisera to compare expression levels in the wild-type (WT) and Kv1.3 null mice (−/−).

(C) Line densitometry was performed within single Western blots to determine pixel density for a visualized protein in the wild-type and null condition. Immunodensity ratio was calculated as the pixel density of the protein in the null mouse over that of the wild-type mouse for proteins exposed on the same piece of nitrocellulose. Mean pixel ratios are plotted ± SEM; sample sizes as indicated represent number of NP40 extractions or isolated membrane preparations. Ratio value of 1.0 (dashed line) indicates no difference in expression. *, Significantly different by Student's t test with arc-sin transformation for percentage data, $\alpha \leq 0.05$. □, not significantly different; ■, significantly different.

was increased in the Kv1.3 null mice only for a period of 12 hr following introduction to a metabolic testing chamber, and, after adapting to the new environment, there was no significant difference in metabolism monitored continuously over 8 days (Supplemental Figure S1D and Table 1). Interestingly, even though total intake was equivalent, the null animals ate more frequently and drank less often when monitored for 8 days as determined by breakage of a photobeam or lickometer to achieve food or water (Table 1).

Kv1.3 null mice were interbred without any obvious lack of breeding success defined in percentage of matings resulting in pregnancy or size of the litter in comparison to wild-type controls. Crosses maintained for the complete 4 day cycle of estrus resulted in pregnancy in 64% of the matings for wild-type animals ($n = 94$) compared with 66% for those from the null mice ($n = 73$). Likewise, the mean litter size was not significantly different between that of wild-type and Kv1.3 null mice (6.5 ± 0.3 [$n = 60$] +/+ versus 6.4 ± 0.3 [$n = 48$] −/−; Student's t test, $\alpha \leq 0.05$).

No apparent differences were observed in the ability of the Kv1.3 null mice to mate or to nurse their offspring, two olfactory-related behavioral tasks. However, in testing for general anosmia where animals are required to retrieve a hidden food item that they smell under the bed litter, Kv1.3 null mice were surprisingly able to outperform the wild-type mice (Figure 5A, Student's t test, $\alpha \leq 0.05$). In fact, in trials utilizing solely naive mice, the retrieval time for Kv1.3 null mice to recover the hidden

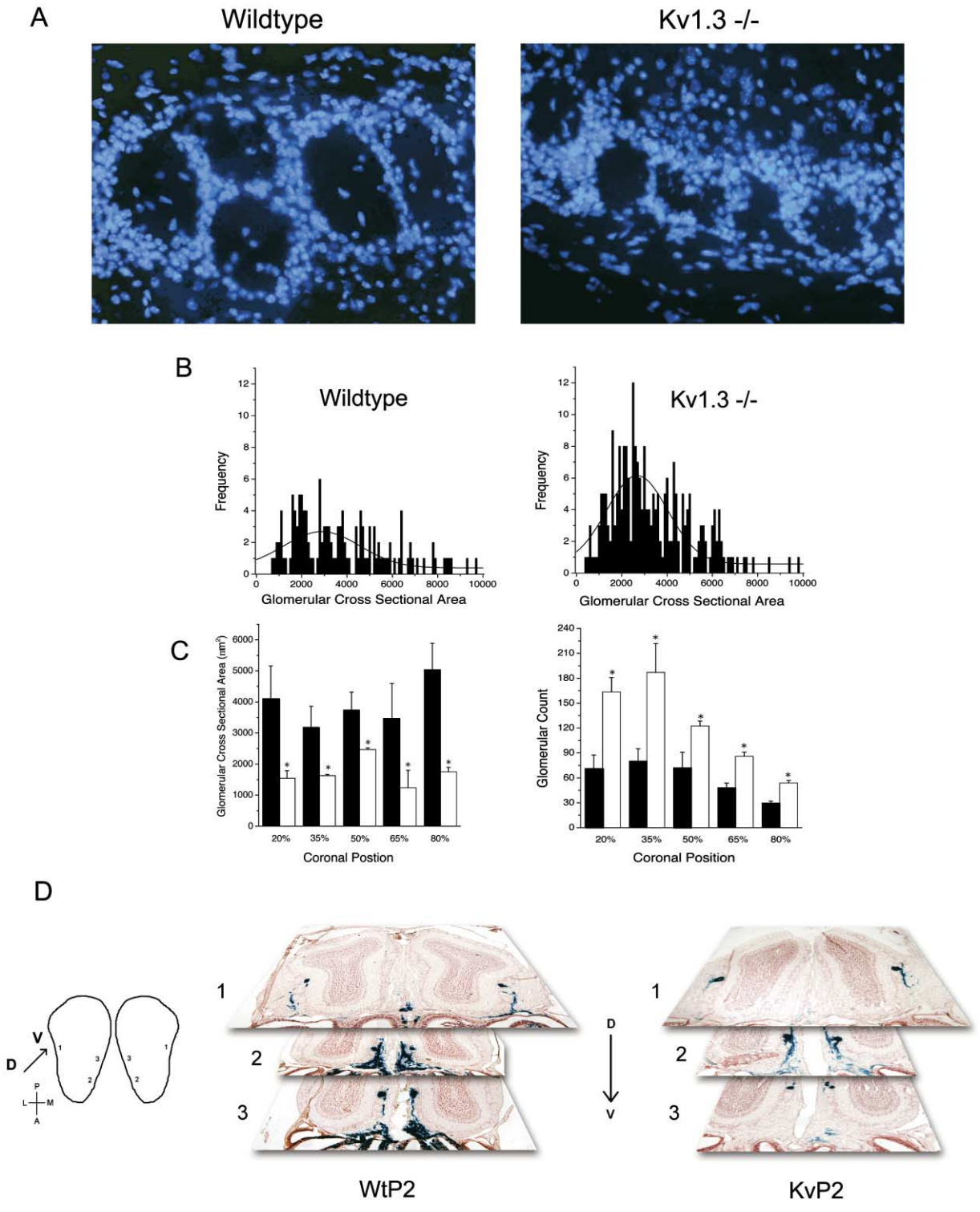

Figure 8. Glomerular Size and Abundance and OB Axonal Targeting in Wild-Type versus *Kv1.3*$^{-/-}$ Mice

(A) Ten micron cyrosections from P10 mice labeled with DAPi nuclear stain to visualize the periglomerular cells circumferentially delineating the boundary of individual glomeruli of wild-type and *Kv1.3*$^{-/-}$ mice.

(B) Image analysis of cresyl violet-stained coronal sections of the olfactory bulb was used to calculate cross sectional area of the glomeruli. The plotted frequency histogram of the glomerular area was fitted by a Gaussian distribution (see Experimental Procedures) to determine the mean area at that coronal position. Graphs demonstrate representative glomeruli areas taken for one wild-type and one *Kv1.3*$^{-/-}$ mouse at the 50% coronal location.

(C) (Left) Histogram plot of the mean glomerular cross sectional area at the 20th, 35th, 50th, 65th, and 80th percentile depth into the OB. ■, wild-type; □, *Kv1.3*$^{-/-}$ mice. Plotted are mean ± SEM, sample sizes (n) ranged from 3–6 non-littermate animals, with statistical significance defined

food item was over twice as fast as that recorded for the wild-type mice, but equally fast as that of wild-type mice when the item was a play item (marble) without an associated odor (Figure 5A).

Odor-habituation trials were then performed to determine whether null animals could distinguish between two odor qualities or whether total olfactory sensation was simply elevated without regard to discrimination or tuning. In the first set of odor-habituation experiments, the odor pairs were comprised of complex odorant mixtures such as peppermint, ground food extract, ground fecal matter extract, or geranyl acetate (GA). Both genotypes had comparably shaped habituation curves when exploratory time was monitored for an odor-saturated cotton swab that was repeatedly presented to the naive animal (see Experimental Procedures) (Figure 5B). Kv1.3 null mice, however, habituated slightly faster than the wild-type animals even though the extent of habituation was similar (Figure 5B, inset). Upon presentation of the novel, second odorant in the pair to determine discrimination from the first, habituated odor quality, Kv1.3 null mice had an increased mean exploratory time between 4- and 30-fold dependent upon the tested odorant pair (Figure 5C). An increased exploratory time following habituation is indicative of the animal's ability to detect the new odor mixture or molecule as different. In contrast, wild-type animals habituated similarly but had far less discrimination ability as reflected in their 1.5- to 2.5-fold increase in exploration time to the novel odorant following habituation. In the second set of odor-habituation experiments, the same experimental paradigm was performed, but now using test odorant pairs of alcohol molecules that differed by only one to four carbons in chain length (Figure 5D). Both Kv1.3 null and wild-type animals had the ability to discriminate odorant molecules differing in one to four C atoms; however, the Kv1.3 null mice outperformed the wild-type mice in alcohol pairs that differed by 1C or 4C in length. Mice of both genotypes performed equally well in discrimination between alcohol molecules that were intermediate in chain length differences (2 or 3 C) (Figure 5D).

Odor-habituation experiments rely on measurement of basal locomotor activity (Table 1) and, more importantly, on exploratory behavior. Even though the equal retrieval time for an unscented object (marble) (Figure 5A) serves as a crude control for random movement of the animal while exploring, we carried out further control measurements of total locomotor and exploratory activity. Total locomotor activity, measured in meters, was determined over 8 days using a custom-designed force platform that centers the animal's home chamber upon a freely rotating ball bearing to calculate movement (Williams et al., 2003). Compared to wild-type mice, Kv1.3 null animals exhibited increased total activity, which was statistically significant during the dark cycle but not during the light cycle (Table 1, Figure 6A) when the behavioral assays were performed. Moreover, when the two groups of animals were monitored for motivation to explore a novel object, their duration of exploration was not significantly different (Figure 6B), thereby strongly validating the difference between the animals on odor-habituation trials.

Last, because the Kv1.3 null mice had an apparent increased ability to discriminate odors, we questioned whether there was a difference in odor-detection threshold in the null mice. Unlike the tests in Figure 5 that utilize naive mice, most traditional behavioral paradigms for odor threshold involve memory, so we first demonstrated that the wild-type and Kv1.3 null mice had equivalent memory recognition of objects after 1 and 24 hr (Figure 6C). This served as a control for the odor-detection experiments that require the trained mouse to retain information learned during the previous day's behavioral session. Using a two-choice paradigm, ten animals of each genotype were trained to dig for a food reward hidden under peppermint-scented litter. Kv1.3 null mice consistently outperformed the wild-type mice by accurate retrieval of the hidden reward item at odorant concentrations that ranged between 1,000- to 10,000-fold less than that found accurately by the wild-type mice (Figure 6D). Both genotypes had similar ability to learn the trained task, as evidenced by the ability of all mice to have the same accuracy in selection (percent correct) at higher odorant concentrations. Number of decisions prior to correct choice was also scored but did not indicate any marked difference between genotypes (data not shown). The only perceived difference we observed, beyond that of odor detection threshold, is that the null mice took longer to make a correct choice at the highest odorant concentrations (Figure 6E).

Loss of Kv1.3 Alters the Expression of Kv1.3 Modulatory and Scaffolding Proteins

To verify further the loss of Kv1.3 transcription in the Kv1.3 null mice (−/−), RT-PCR was conducted with RNA from the OB of P20 null and wild-type mice. Agarose gel electrophoresis of the PCR-amplified products confirmed a band of predicted size in wild-type animals, and this band was missing in the Kv1.3 null animals (Figure 7A, left). We also confirmed the lack of immunoreactive Kv1.3 protein in the OB of Kv1.3 null mice. Using a previously characterized antiserum for the Kv1.3 channel (Tucker and Fadool, 2002), the expression of the channel protein could only be demonstrated in wild-type but not in null mice (Figure 7A, right).

Kv1.3 is the target for multiple tyrosine kinase signaling cascades and its function is altered through participation in several protein-protein interactions with SH3, SH2, and PTB containing scaffolding and adaptor molecules. We hypothesized that its absence might perturb the expression or proportion of scaffolding and modulatory kinases that normally associate with it. Purified

at the 95% confidence level (*) for each coronal position, Student's t test. (Right) Same as in (C), left, except for mean glomeruli number. (D) The distribution of olfactory neurons expressing the P2 odorant receptor protein was visualized in coronal cyrosections in P2-IRES-tau-LacZ transgenic mice (WtP2) versus Kv1.3 null P2-IRES-tau-LacZ double homozygous mutant mice (KvP2). Sections were processed using X-gal histochemistry and counterstained with neutral red. Although there is some interanimal variability (five animals analyzed of each genotype), the location of axonal projection and number of targeted glomeruli was not qualitatively different in the Kv1.3 null background.

membrane preparations or NP40 solubilized lysates were separated by SDS-PAGE and electrotransferred to nitrocellulose in order to probe for known membrane bound or cytosolic modulatory or associated proteins of Kv1.3 in the OB. Representative nitrocellulose blots labeled for these various channels, kinases, and adaptor proteins are shown in Figure 7B. Quantitative immunodensity measurements (Figure 7C) demonstrate that the neurotrophin receptor TrkB, the cellular kinase Src, a voltage-gated Ca channel (CaPan), the adaptor proteins 14-3-3, nShc, PSD-95, and Grb, as well as total tyrosine phosphorylation in the Kv1.3 null mice, are elevated over levels in wild-type mice. In contrast, other types of voltage-gated ion channels (Kv1.4, Kv1.5, ClC_2, ClC_3, NaPan), the receptor tyrosine kinase insulin receptor, and the adaptor protein ras do not have significantly altered total protein expression levels across the two genotypes.

Structural Changes in the Olfactory Bulb of Kv1.3 Null Mice

The TrkB receptor is elevated in Kv1.3 null mice. It is known that activation of this receptor by BDNF is dependent upon neural activity and that it regulates axonal growth. We therefore questioned whether there was an anatomical change in the OB that might explain the increased ability of these animals to detect odorant molecules. In comparing the structure and size of the neuroepithelial layers of the OB in P10 animals for each genotype, we found that the only significant alterations were restricted to the glomerular layer (Figure 8A). Although glomerular size increases with age until approximately 12 weeks (Pomeroy et al., 1990) and is greatest at the midpoint of the bulb (Royet et al., 1988), the mean glomeruli size sampled at the midpoint of the OB from wild-type mice was within the range reported for other rodent species (LaMantia et al., 1992). Species comparisons of mean cross sectional areas were recalculated from the midpoint of the bulb from diameters reported in the literature using πr^2 as an approximation as follows: mouse (P10) mean glomeruli size in this study = 3455 μm^2, mouse (P60) reported by Royet et al. (1988) = 5027 μm^2, rat (P60) reported by Meisami and Safari (1981) = 3849 μm^2, and bat reported by Abercrombie (1946) = 5027 μm^2. In contrast, the mean glomeruli size of Kv1.3 null mice was significantly smaller than that of wild-type mice (2882 $\pm$ μm^2 $-/-$ versus 3455 $\pm$ μm^2 $+/+$, Student's t test, $\alpha \leq 0.05$) (Figure 8B).

Because the size and number of glomerular units depend on position within the olfactory bulb, we elected to calculate the size and abundance of glomeruli at five equally spaced coronal locations across the bulb. Three non-littermates of each genotype (P10) were used in the study. Individual glomeruli were hand circled using the Metamorph image analysis program, the glomerular cross sectional area was binned in increments of 100 μm^2, and then the plotted histogram distribution was fit with a Gaussian function ($y = y_o + Ae^{-[(x - xc)2/2w2]}$, where A = amplitude, w = width, y_o = y offset) to determine the mean glomeruli size per genotype at that location. Although size and number of glomeruli did vary with location, the Kv1.3 null mice had glomeruli that were significantly smaller (representing a decrease range of 37%–58%) and more numerous (with an increase range of 170%–240%) than those of wild-type mice at all locations (Figure 8C).

Because of the striking finding of an increased number of smaller glomeruli, we tested the hypothesis that axonal projections are altered by crossing the Kv1.3 null mice with mice in which a single odorant receptor called P2 is linked to the expression of lacZ-tagged tau protein (Mombaerts et al., 1996; Schaefer et al., 2001). Visualization of the axonal projections from olfactory sensory neurons containing the P2 receptor protein using β-galactosidase did not reveal any obvious differences in staining of the P2 glomerulus between wild-type and *Kv1.3*$^{-/-}$ animals (Figure 8D).

Discussion

We have demonstrated that mice deficient in the voltage-dependent potassium channel Kv1.3 have a heightened sense of smell and distinct alterations of the structure of the olfactory bulb and its protein composition. Mitral cells of Kv1.3 null mice fail to exhibit normal modulation of currents by receptor tyrosine kinases, and their potassium currents are of lower amplitude and have modified kinetic properties. Changes in the potassium current undoubtedly contribute to the altered pattern of firing in response to depolarization in the Kv1.3 null neurons. It is likely that the changes in calcium channel expression (Friedman and Strowbridge, 2000), together with altered levels of interacting proteins, also influence the resultant pattern of firing. Interestingly, B.W. Strowbridge et al. (submitted) find that application of MgTx to rat mitral cells abolishes action potential clustering and results in tonic firing at an increased average frequency. Therefore, loss of Kv1.3 may serve to provide more spiking precision underlying repetitive stimulation by eliminating periodity or clustering to increase firing frequency.

The axonal processes of the olfactory sensory neurons synapse onto the mitral cell at the level of the glomeruli, representing the first processing of olfactory information at the level of the central nervous system (see Korsching, 2002; Nagao et al., 2002). The increased ability of Kv1.3 null mice, both to sense olfactory cues and to discriminate between structurally similar molecules, could be related either to the structural changes at the level of the glomeruli or to alterations in the intrinsic excitability of olfactory neurons. For example, greater regularity in firing in the Kv1.3 null OB neurons may alter the pattern of response to olfactory information. Our current-clamp recordings suggest that less current is required to elicit spike frequencies equivalent to that of wild-type neurons, a property that may allow the animals to detect odor molecules at lower concentrations. Alternatively, the formation of smaller and more numerous units for this type of processing may provide a greater resolving power to improve odorant discrimination and threshold detection. This may be tied, for example, to the elevated trkB receptor expression in the Kv1.3 null mice, which has been demonstrated to increase activity-dependent growth of axonal projections (Balkowiec and Katz, 2002). There is precedence in the visual system for modulation of axonal projections by changes in channel

activity during critical periods of development (McFarlane and Pollack, 2000). Although our results in the KvP2 double mutant mice demonstrate lack of altered projection to one type of glomerulus (P2), it is estimated that there are approximately 1000 odor receptor genes (and only three lines of receptor-tagged transgenic mice have been created: P2, M71, M72) (Mombaerts et al., 1996; Bozza et al., 2002; Potter et al., 2001). Thus, the lack of finding additional P2 glomeruli in the KvP2 double mutant mice may be inherently biased. Although animal variability in the position and number of P2 glomeruli has been reported (Royal and Key, 1999; Schaefer et al., 2001), there are two additional important factors: (1) the odorant ligand that activates the P2 receptor is undetermined, and we do not know the importance of P2 for odor sensitivity; and (2) projection to these glomeruli demonstrates lack of plasticity and is unchanged in CNG channel null mice that are virtually anosmic (Zheng et al., 2000). It will thus be important for future studies to investigate the cellular mechanism underlying the Kv1.3 null mice phenotype. Generation of KvM71 and KvM72 double mutant mice is one approach, but it will be equally valuable to explore subtle changes in connectivity. Kv1.3 null mice could be bred to YFP-expressing mitral cell mice (Feng et al., 2000) to visualize connections of olfactory sensory neurons, in general, to the mitral cells at the smaller glomeruli. Retrograde glomeruli tracing, as recently reported by Lodovichi et al. (2003), would be an excellent method to determine if all glomeruli of Kv1.3 null mice are physically wired. Last, we plan to stereotaxically deliver MgTx into the OB of adult wild-type animals to explore the reproducibility of the behavioral, electrical, and biochemical phenotype, independent of the glomerular structural changes.

An additional possibility that cannot be ruled out by our experiments is that the site for enhanced olfactory performance resides in neural structures other than the OB. Even though Kv1.3 has a highly restrictive pattern of expression in the CNS, it is found in the dendate gyrus of the hippocampus. Application of pharmacological blockers of Kv1.1 and Kv1.3 into the third ventricle improves associative learning in rats (Kourrich et al., 2001). Since the deletion of Kv1.3 is not restricted to the OB, it is possible that these mice are simply "smarter." Nevertheless, our experiments make this possibility less likely for several reasons. Mice used in the anosmia screen and odor habituation experiments were naive, and the capacity for learning did not factor into the behavioral task employed. Moreover, there was no effect of Kv1.3 elimination on the retrieval of a marble or the observation of a novel object, which were used as motivational tasks (play), and which might have been expected to change if hippocampal activity had been significantly altered after deletion of Kv1.3. Finally, tasks that required memory (object recognition) or trained behaviors did not demonstrate any difference after deletion of Kv1.3.

Previous work in heterologous expression systems has clearly shown that there is reciprocal regulation of the level of expression of the Kv1.3 channel and the kinase pathways that modulate its function. For example, Src kinase causes suppression of Kv1.3 current, but expression of Kv1.3 downregulates the expression of the kinase (Holmes et al., 1997). Activation of the insulin receptor suppresses Kv1.3 current, and, although expression of Kv1.3 does not alter levels of the insulin receptor, it alters its ability to be tyrosine phosphorylated (D.A.F., unpublished data). In addition, we have recently demonstrated that, while activation of TrkB causes suppression of Kv1.3 current, coexpression of Kv1.3 with TrkB causes a strong upregulation in the expression of the channel protein, even in the absence of activation of TrkB by BDNF (Colley et al., 2004). Consistent with these observations in cell lines, we found that deletion of Kv1.3 produced increases in the expression levels of CaPan, TrkB, Src, Grb, 14-3-3, Shc, PSD-95, and of total tyr phosphorylation levels. As increased tyrosine phosphorylation results in the suppression of the current of many Kv family members (Huang et al., 1993; Holmes et al., 1996a, 1996b; Nitabach et al., 2002) and may modulate the remaining Kv1.4 or Kv1.5 channels, these biochemical changes may contribute to the lower peak current magnitude and slower τ_{Inact} in the Kv1.3 null mice.

The major function of voltage-dependent potassium channels is to regulate potassium flux across the plasma membrane to shape the excitability of neurons. It appears, however, that the role of the Kv1.3 channel may be more far-reaching than can be accounted for simply by its effects on membrane potential. Our findings have indicated that this channel subunit influences the balance of multiple signaling molecules in the olfactory bulb and that it plays an important role in its normal development and in the function of olfactory discrimination. Our data suggest that, in addition to its role in the control of excitability, the Kv1.3 channel subunit is a central signaling molecule through which signal transductory and modulatory proteins interact to regulate intercellular communication in neurons.

Experimental Procedures

Solutions and Antibodies

The composition of olfactory bulb neuron (OBN) patch pipette and bath recording solutions, nonidet-P40 protease and phosphatase inhibitor (NP40 PPI) solution, homogenization buffer (HB), and phosphate buffered saline (PBS) are as described in Tucker and Fadool (2002). Human recombinant brain-derived neurotrophic factor (BDNF) was purchased from Promega (Madison, WI), and human recombinant insulin was purchased from Boehringer Mannheim (Indianapolis, IN). Margatoxin (MgTx), a selective blocker of Kv1.3, was a generous gift from Dr. Reid Leonard, Merck Research Laboratories (Rahway, NJ), and 5-nitro-2-(3-phenylpropyl-amino) benzoic acid (NNPB), a nonselective blocker of Cl channels, was purchased from Sigma.

The previously characterized AU13 antiserum against Kv1.3 was used for immunoprecipitation (1:1000) and Western blot detection (1:1500) of Kv1.3 in the OB (Tucker and Fadool, 2002). Tyrosine phosphorylated proteins were detected on Western blots (1:1000) with the mouse monoclonal antibody 4G10 (Upstate Biotechnology, Inc., Lake Placid, NY). The following additional antisera were used to screen expression of channels, kinases, and scaffolding proteins in the OB of wild-type versus Kv1.3 null mice by Western blot at the following dilutions: TrkB (1:800; monoclonal #47; BD Biosciences, San Diego, CA), Kv1.4 (1:1000; polyclonal, gift from Dr. J.O. Dolly), Kv1.5 (1:1000; polyclonal, gift from Dr. T.C. Holmes), ClC2/ClC3 (1:200; polyclonal GST fusion proteins, Alomone Laboratories, Jerusalem, Israel), NaPan (1:500; monoclonal #SP-19, Sigma Chemical), CaPan (1:200, Alomone Laboratories), IR (1:1000; polyclonal GST fusion protein, Upstate), Src (1:80; monoclonal #327, Oncogene Research Products, Cambridge, MA), Grb (1:1000, polyclonal #K-20,

Santa Cruz Biotechnology, Santa Cruz, CA), nShc (1:500 polyclonal #H-108, Santa Cruz), Ras (1:500; monoclonal #18, BD Biosciences), and 14-3-3 (1:1000 monoclonal #12, BD Biosciences).

Alcohol odorants (ethyl butyrate [C6], ethyl valerate [C7], ethyl heptanoate [C9], and ethyl caprylate [C10]) were obtained as 99% purity grade from Aldrich Chemical Co. (Milwaukee, WI). Geranyl acetate (GA) was 98% purity grade from Sigma. Peppermint extract was obtained at Publix groceries (Tallahassee, FL), UPC 0-5210007079-7, and food extract was prepared from General Laboratory Diet 5001 (Purina). Liquid odorants were diluted to working concentrations with light mineral oil (Fisher; Cat. 0121-1) and vortexed for 10 s. For odor habituation experiments, 10 μl of diluted odorant was applied directly to a cotton swab for behavioral testing. For odorant threshold testing, 500 μl of diluted odorant was applied to 20 g of crushed walnut chips to scent the litter. Feces were obtained from lactating female, caecotroph matter. Solids, the food chow, and the feces, respectively, were crushed between paper with pressure applied, and a mineral oil-wetted swab was rolled in the resulting crumbs for behavioral testing.

Biochemistry

Postnatal day (P), twenty mice were euthanized by CO_2 inhalation as per Florida State University Laboratory Animal Resources and AVMA-approved methods, and olfactory bulbs (OBs) were quickly harvested after decapitation. OBs were immediately homogenized in HB or NP40 PPI for fifty strokes with a Kontes tissue grinder (size 20) on ice. HB processed bulbs were used to isolate membrane proteins while NP40 PPI processed bulbs were used to extract cytosolic proteins as previously described (Tucker and Fadool, 2002).

Membrane or cytosolic proteins (25 μg/lane) were separated on 8%–10% acrylamide gels by SDS-PAGE and electrotransferred to nitrocellulose blots as previously described (Cook and Fadool, 2002; Tucker and Fadool, 2002). Enhanced chemiluminescence (ECL; Amersham-Pharmacia) exposure on Fugi Rx film (Fisher) was used to visualize labeled proteins. The film autoradiographs were analyzed by quantitative densitometry using a Hewlett-Packard PhotoSmart Scanner (model 106-816, Hewlett Packard, San Diego, CA) in conjunction with Quantiscan software (Biosoft, Cambridge, England). Immunodensity ratios (*Kv1.3*−/− over wild-type) were calculated, normalized, and analyzed as described previously (Tucker and Fadool, 2002).

Electrophysiology

Cultured OBNs were prepared as previously described for rat (Tucker and Fadool, 2002) and slightly modified for mice (Colley et al., 2004). OBNs were voltage or current clamped at room temperature in the whole-cell recording configuration. Electrodes were fabricated from Jencons glass (Cat #M15/10, Jencons Limited, Bedfordshire, England), fire-polished to approximately 1 μm tip diameter, and coated near the tip with beeswax to reduce the electrode capacitance. Pipette resistances were between 9 and 14 MΩ. All voltage signals were generated, and data were acquired using an Axopatch 200B in conjunction with pClamp8.0 software (Axon Instruments, Foster City, CA). The amplifier output was filtered at 2 kHz and digitized at 2–5 kHz.

All electrophysiological data were analyzed using pClamp software (Axon Instruments). Data traces were subtracted linearly for leakage conductance. The inactivation of the macroscopic current (τ_{inact}) was fit to the sum of two exponentials [$y = y_0 + A_1\exp(-x/\tau_1) + A_2\exp(-x/\tau_2)$] by minimizing the sums of squares, where y_0 was the Y offset, τ_1 and τ_2 were the inactivation time constants, and A_1 and A_2 were the amplitudes. The two inactivation time constants (τ) were combined by multiplying each by its weight (A) and summing as described previously (Fadool et al., 2000).

Odor Habituation

To test for general anosmia, naive mice were removed from the home cage and placed in a testing cage (29.2 × 19.1 × 12.7 cm) in which a peanut butter cracker or size-matched marble was hidden from view under the litter. The item to be retrieved was randomly selected and hidden in a different location in the cage on each trial. The retrieval time was recorded from the instant the mouse was released in the center of the cage until the item was found. Experiments were terminated at 600 s (10 min), and mice were scored that time duration if the item was not retrieved.

Odor-habituation paradigms were slightly modified from that devised previously by Fletcher and Wilson (2002). To test for discrimination of a second odor following the habituation to a first odor, naive mice were removed from the home cage and again placed in a similar-sized testing cage. Odor mixtures or single odorant molecules differing by number of carbon atoms were diluted 1:100 in mineral oil and applied to a cotton swab. The cotton swab was introduced to the mouse through the top of the testing cage and time of active investigation/smelling of the odor was recorded. Mice were habituated to the first odor of an odor pair combination by repeat stimulation with the odor saturated swab for seven trials using 1 min resting intervals. On the eighth trial, the second odor of the odor pair was presented and time of increased exploration was scored. All recorded times were normalized and compared to the animal's original exploration time prior to habituation to minimize the between-animal variance. The ratio of normalized exploratory time on the seventh trial (habituated) over that of the eighth trial (new odorant) was compared across wild-type and *Kv1.3*$^{-/-}$ mice within an odorant pair using an arc-sin transformation for percentage data with a paired t test at the 95% confidence level.

Odorant Threshold

Twenty mice (ten of each genotype) were introduced to a two-choice discrimination apparatus (one waiting room and two choice compartments) (Colacicco et al., 2002) for a 3 day habituation period followed by a 1 week training period. Commencing with the habituation period, mice were placed on a limited food schedule of 2–3 g/day with water available ab libitum. Body weight was taken daily and food amount adjusted to maintain all animals at 85% of free-feeding body weight. During the habituation period, mice were introduced to 3 inch diameter feeding cups filled with 20 g crushed walnut chips (Petco, lizard bedding) scented with 1:10 peppermint extract and baited with visible 1–2 pieces of honey-flavored cereal on top of the digging medium (walnut chips). During the training period, mice were presented with two feeding cups, one containing scented and the other unscented walnut chips. Both feeding cups were baited with the hidden food reward, only the unscented chips had the reward placed under a metal screen fitted inside the feeding cup (inaccessible) and the scented chips had the reward on top of the screen. Mice were trained to dig for the food reward by odorant pairing and were immediately removed to the waiting room to terminate the trial if they dug in the unscented chips (wrong decision).

Odorant threshold testing began when performance levels reached 100% correct choice for the 1:10 peppermint dilution (step 1 on scale; Figure 5D). For each daily test session, mice were progressively tested on sequentially lower dilutions that were prepared in 10-fold dilution step increments. A test of a given dilution consisted of four to eight trials. If a mouse responded with 80%–100% for correct decisions, it was tested on the next lower dilution. Since mice only had the capacity to stay attentive to the task for 30–45 min (approximately fifteen trials), the lowest dilution at which 100% correct decisions were made was resumed on the next day. If the mouse responded incorrectly (60%–80% correct decisions), it was retested twice with the previous stronger dilution. Odorant threshold was determined at 50% correct decisions or retrieval of reward by chance alone. All training and testing were conducted between 1600 and 2000 hr in a room isolated from external noise. This behavioral paradigm was designed based upon modification of protocols described in Yee and Wysocki (2001), Colacicco et al. (2002), and the Hyde Laboratory (Schering Plough Research Institute, Kenilworth, New Jersey).

Object Recognition

Eighteen mice were individually habituated for 1 week in an open-field chamber (26 × 47 × 13.5 cm) prior to performing the task. For the recognition testing, two objects were placed in the chamber and mice were allowed to explore them for a 5 min interval. The amount of time the mouse was oriented to each object within one head length was scored. After either 1 or 24 hr, mice were tested for memory retention by replacing two objects in the chamber at

the same position, but replacing object 2 (familiar object) with object 3 (novel object) and again scoring orientation for a 5 min interval. This behavioral paradigm was designed based upon that described in Jeon et al. (2003).

Whole-Animal Physiology Monitoring

Twenty mice of each genotype were monitored for 8 days in shoebox cages (26 × 47 × 13.5 cm) custom modified for continuous determination of oxygen consumption, locomotor activity, and ingestive behaviors (Williams et al., 2003). Briefly, cages were placed inside environmental chambers that provided computer control of ambient temperature (T_a = 23°C) and light cycles. Mixed cage air was sampled for 30 s every 4 min, dried, and compressed prior to reaching gas analyzers to determine VO_2. Stiff strain-gauge load beam transducers were attached under two adjacent corners of the cage platform and sampled at 50 Hz to measure changes in the chamber's center of gravity (resolution = 1 mm), allowing localization of the mouse's position in two dimensions. Locomotor activity was defined as unidirectional movement greater than 1 cm and cumulated for dark and light phases. Feeding behavior was monitored by a photobeam sensor across the entrance to the feeder, which was filled with powdered chow (Purina 5001; 3.3 kcal/g) and had a 50 ms resolution. Water bottles were positioned in a lick block instrumented to measure contact at the bottle's spout.

Glomerular Analysis

Three sets of serial, coronal OB sections (each 12 μm) from P10 wild-type and Kv1.3 null mice were prepared as previously (Fadool et al., 2000). Sections were stained with cresyl violet for suitable visualization of the glomeruli by light photomicroscopy (Zeiss Axiovert S 100). Digital images were captured using a Zeiss Axiocam digital camera and AxioVision Software. Number and cross sectional area of glomeruli were computed using Metamorph (v5.051) in conjuction with Orgin (v6.0) software. The last section of each serial set was determined as the first section without glomeruli. The expected 20th, 35th, 50th, 65th, and 80th percentile sections for each bulb were calculated from this information. In situations where the section to be photographed for analysis was not in suitable condition to be used, the section either immediately before or after it was substituted.

Acknowledgments

We would like to thank the following undergraduate volunteers for assistance with behavioral experiments, mouse colony maintenance, and routine genotyping: Mr. Matt Edsall, Ms. Dietra Haynes, Mr. Dan Otten, Mr. Grant Richards, and Mr. Chad Thorson. We would like to thank Mr. David Watson and XiXi Jia for technical assistance with cryosectioning; Dr. Michael Meredith and Ms. Jessica Brann for histological assistance; Ms. Rani Dhanarajan for assistance with RNA handling; Ms. Jill Scarbourough for technical assistance; and Drs. Marc Freeman and James Fadool for access to image analysis and photomicroscopy equipment, respectively. We are grateful to Drs. Ben Strowbridge, James Fadool, Laura Blakemore, and Paul Trombley for very helpful discussions; and Drs. Hanno Wurbel and Lynn Hyde for valuable insight into the design of our mouse behavioral assays. This work was supported by NIH grants DC03387 (NIDCD, D.A.F.) and DC01919 (NIDCD, L.K.K). R.A.F. is an investigator of the Howard Hughes Medical Institute.

Received: May 7, 2003
Revised: October 6, 2003
Accepted: December 15, 2003
Published: February 4, 2004

References

Abercrombie, M. (1946). Estimate of nuclear population from microtome sections. Anat. Rec. *94*, 239–247.

Balkowiec, A., and Katz, D.M. (2002). Cellular mechanisms regulating activity-dependent release of native brain-derived neurotrophic factor from hippocampal neurons. J. Neurosci. *22*, 10399–10407.

Bowlby, M.R., Fadool, D.A., Holmes, T.C., and Levitan, I.B. (1997). Modulation of the Kv1.3 potassium channel by receptor tyrosine kinases. J. Gen. Physiol. *110*, 601–610.

Bozza, T., Feinstein, P., Zheng, C., and Mombaerts, P. (2002). Odorant receptor expression defines functional units in the mouse olfactory system. J. Neurosci. *22*, 3033–3043.

Cayabyab, F.S., Khanna, R., Jones, O.T., and Schlichter, L.C. (2000). Suppression of the rat microglia Kv1.3 current by *src*-family tyrosine kinases and oxygen/glucose deprivation. Eur. J. Neurosci. *12*, 1949–1960.

Colacicco, G., Welzl, H., Lipp, H.P., and Wurbel, H. (2002). Attentional set-shifting in mice: modification of a rat paradigm, and evidence for strain-dependent variation. Behav. Brain. Res. *132*, 95–102.

Colley, B., Tucker, K., and Fadool, D.A. (2004). Comparison of modulation of Kv1.3 channel by two receptor tyrosine kinases in olfactory bulb neurons of rodents. Recept. Channels *10*, 1–12.

Cook, K.K., and Fadool, D.A. (2002). Two adaptor proteins differentially modulate the phosphorylation and biophysics of Kv1.3 ion channel by SRC kinase. J. Biol. Chem. *277*, 13268–13280.

Fadool, D.A., and Levitan, I.B. (1998). Modulation of olfactory bulb neuron potassium current by tyrosine phosphorylation. J. Neurosci. *18*, 6126–6137.

Fadool, D.A., Holmes, T.C., Berman, K., Dagan, D., and Levitan, I.B. (1997). Multiple effects of tyrosine phosphorylation on a voltage-dependent potassium channel. J. Neurophysiol. *78*, 1563–1573.

Fadool, D.A., Tucker, K., Phillips, J.J., and Simmen, J.A. (2000). Brain insulin receptor causes activity-dependent current suppression in the olfactory bulb through multiple phosphorylation of Kv1.3. J. Neurophysiol. *83*, 2332–2348.

Feng, G., Mellor, R.H., Bernstein, M., Keller-Peck, C., Nguyen, Q.T., Wallace, M., Nerbonne, J.M., Lichtman J.W., and Sanes, J.R. (2000). Imaging neuronal subsets in transgenic mice expressing multiple spectral variants of GFP. Neuron *28*, 41–51.

Fletcher, M.L., and Wilson, D.A. (2002). Experience modifies olfactory acuity: acetylcholine-dependent learning decreases behavioral generalization between similar odorants. J. Neurosci. *22*, 1–5.

Friedman, D., and Strowbridge, B.W. (2000). Functional role of NMDA autoreceptors in olfactory mitral cells. J. Neurophysiol. *84*, 39–50.

Holmes, T.C., Fadool, D.A., Ren, R., and Levitan, I.B. (1996a). Association of src tyrosine kinase with a human potassium channel mediated by SH3 domain. Science *274*, 2089–2091.

Holmes, T.C., Fadool, D.A., and Levitan, I.B. (1996b). Tyrosine phosphorylation of the Kv1.3 potassium channel. J. Neurosci. *16*, 1581–1590.

Holmes, T.C., Berman, K., Swartz, J.E., Dagan, D., and Levitan, I.B. (1997). Expression of voltage-gated potassium channels decreases cellular protein tyrosine phosphorylation. J. Neurosci. *17*, 8964–8974.

Huang, X.Y., Morielli, A.D., and Peralta, E.G. (1993). Tyrosine kinase-dependent suppression of a potassium channel by the G protein-coupled m1 muscarinic acetylcholine receptor. Cell *75*, 1145–1156.

Jeon, D., Yang, Y.M., Jeong, M.J., Philipson, K.D., Hyewhon, R., and Shin, H.S. (2003). Enhanced learning and memory in mice lacking Na/Ca Exchanger 2. Neuron *38*, 965–976.

Jonas, E.A., and Kaczmarek, L.K. (1996). Regulation of potassium channels by protein kinases. Curr. Opin. Neurobiol. *6*, 318–323.

Jugloff, D.G.M., Khanna, R., Schlichter, L.C., and Jones, O.T. (2000). Internalization of the Kv1.4 potassium channel is supressed by clustering interactions with PDS-95. J. Biol. Chem.*275*, 1357–1364.

Kim, E., Niethammer, M., Rothschild, A., Jan, Y.N., and Sheng, M. (1995). Clustering of *Shaker*-type K+ channels by interaction with a family of membrane-associated guanylate kinases. Nature *378*, 85–88.

Koni, P.A., Khanna, R., Chang, M.C., Tang, M.D., Kaczmarek, L.K., Schlichter, L.C., and Flavell, R.A. (2003). Compensatory anion currents in Kv1.3 channel-deficient thymocytes. J. Biol. Chem. *278*, 39443–39451.

Korsching, S. (2002). Olfactory maps and odor images. Curr. Opin. Neurobiol. *12*, 387–392.

Kourrich, S., Mourre, C., and Soumireu-Mourat, B. (2001). Kaliotoxin, a Kv1.1 and Kv1.3 channel blocker, improves associative learning in rats. Behav. Brain. Res. *120*, 35–46.

LaMantia, A.S., Pomeroy, S.L., and Purves, D. (1992). Vital imaging of glomeruli in the mouse olfactory bulb. J. Neurosci. *12*, 976–988.

Lodovichi, C., Belluscio, L., and Katz, L.C. (2003). Functional topography of connections linking mirror-symmetric maps in the mouse olfactory bulb. Neuron *38*, 265–276.

Marom, S., and Levitan, I. (1994). State-dependant inactivation of the Kv3 potassium channel. Biophys. J. *67*, 579–589.

McFarlane, S., and Pollack, N.S. (2000). A role for voltage-gated potassium channels in the outgrowth of retinal axons in the developing visual system. J. Neurosci. *20*, 1020–1029.

Meisami, E., and Safari, L. (1981). A quantitative study of the effects of early unilateral olfactory deprivation on the number and distribution of mitral and tufted cells and of glomeruli in the rat olfactory bulb. Brain Res. *221*, 81–107.

Mombaerts, P., Wang, F., Dulac, C., Chao, S.K., Nemes, A., Mendelsohn, M., Edmondson, J., and Axel, R. (1996). Visualizing an olfactory sensory map. Cell *87*, 675–686.

Nagao, H., Yamaguchi, M., and Mori, K. (2002). Grouping and representation of odorant receptors in domains of the olfactory bulb sensory map. Microsc. Res. Tech. *58*, 168–175.

Nitabach, M.N., Llamas, D.A., Thompson, I.J., Collins, K.A., and Holmes, T.C. (2002). Phosphorylation-dependent and phosphorylation-independent modes of modulation of shaker family voltage-gated potassium channels by SRC family protein tyrosine kinases. J. Neurosci. *22*, 7913–7922.

Pomeroy, S.L., LaMantia, A.-S., and Purves, D. (1990). Postnatal construction of neural circuitry in the mouse olfactory bulb. J. Neurosci. *10*, 1952–1966.

Potter, S.M., Zheng, C., Koos, D.S., Reinstein, P., Fraser, S.E., and Mombaerts, P. (2001). Structure and emergence of specific olfactory glomeruli in the mouse. J. Neurosci. *21*, 9713–9723.

Rivera, J.F., Ahmad, S., Quick, M.W., Liman, E.R., and Arnold, D.B. (2003). An evolutionarily conserved dileucine motif in Shal K^+ channels mediates dendritic targeting. Nat. Neurosci. *6*, 243–250.

Rogalski, S.L., Appleyard, S.M., Pattillo, A., Terman, G.W., and Chavkin, C. (2000). TrkB activation by brain-derived neurotrophic factor inhibits the G-protein-gated inward rectifier Kir3 by tyrosine phosphorylation of the channel. J. Biol. Chem. *275*, 25082–25088.

Royal, S.J., and Key, B. (1999). Development of P2 olfactory glomeruli in P2-internal ribosome entry site-tau-lacZ transgenic mice. J. Neurosci.*19*, 9856–9864.

Royet, J.P., Soouchier, C., Jourdan, F., and Ploye, H. (1988). Morphometric study of the glomerular population in the mouse olfactory bulb: numerical density and size distribution along the rostrocaudal axis. J. Comp. Neurol. *270*, 559–568.

Scannevin, R.H., and Trimmer, J.S. (1997). Cytoplasmic domains of voltage-sensitive K+ channels involved in mediating protein-protein interactions. Biochem. Biophys. Res. Commun. *232*, 585–589.

Schaefer, M., Finger, T.E., and Restrepo, D. (2001). Variability of position of the P2 glomerulus within a map of the mouse olfactory bulb. J. Comp. Neurol. *436*, 351–362.

Tiffany, A.M., Manganas, L.N., Kim, E., Hsueh, Y.-P., Sheng, M., and Trimmer, J.S. (2000). PSD-95 and SAP97 exhibit distinct mechanisms for regulating K+ channel surface expression and clustering. J. Cell. Biol. *148*, 1–147.

Tucker, K., and Fadool, D.A. (2002). Neurotrophin modulation of voltage-gated potassium channels in rat through TrkB receptors is time and sensory experience dependent. J. Physiol. *542*, 413–429.

Williams, T.D., Chambers, J.B., Gagnon, S.P., Roberts, L.M., Henderson, R.P., and Overton, J.M. (2003). Cardiovascular and metabolic responses to fasting and thermoneutrality in A^y mice. Physiol. Behav. *78*, 615–623.

Wong, W., Newell, E.W., Jugloff, D.G.M., Jones, O.T., and Shlichter, L.C. (2002). Cell surface targeting and clustering interections between heterologously expressed PSD-95 and the *Shal* voltage-gated potassium channel, Kv4.2. J. Biol. Chem. *277*, 204223–20430.

Xu, J., Koni, P.A., Wang, P., Li, G., Kaczmarek, L.K., Wu, Y., Li, Y., Flavell, R.A., and Desir, G.V. (2003). The voltage-gated potassium channel Kv1.3 regulates energy homeostasis and body weight. Hum. Mol. Genet. *12*, 551–559.

Yee, K.K., and Wysocki, C.J. (2001). Odorant exposure increases olfactory sensitivity: olfactory epithelium is implicated. Physiol. Behav. *72*, 705–711.

Yellen, G. (2002). The voltage-gated potassium channels and their relatives. Nature *419*, 35–42.

Zheng, C., Feinstein, P., Bozza, T., Rodriguez, I., and Mombaerts, P. (2000). Peripheral olfactory projections are differentially affected in mice deficient in a cyclic nucleotide-gated channel subunit. Neuron *26*, 81–91.